Science and Technology for Energy Transition **78**, 21 (2023)

https://doi.org/10.2516/stet/2023017

Characterization and Modeling of the Subsurface in the Context of Ecological Transition
Yannick Peysson and Jacques Pironon (Guest Editors)

Available online at:
stet-review.org

REGULAR ARTICLE OPEN ACCESS

Quantitative monitoring of dissolved gases in a flooded borehole: calibration of the analytical tools

Van-Hoan Le[1,2], Marie-Camille Caumon[1,*], Jacques Pironon[1], Philippe de Donato[1], Médéric Piedevache[3], Aurélien Randi[1], Catherine Lorgeoux[1], and Odile Barres[1]

[1] Université de Lorraine, CNRS, GeoRessources laboratory, F-54506 Vandœuvre-lès-Nancy, France
[2] University Grenoble Alpes, CEA, LETI, Grenoble, France
[3] Solexperts France, 10 allée de la Forêt de la Reine, 54500 Vandœuvre-lès-Nancy, France

Received: 16 December 2022 / Accepted: 11 July 2023

Abstract. Gas monitoring is a prerequisite to understanding the exchange, diffusion, and migration processes of natural gases within underground environments, which are involved in several applications such as geological sequestration of CO_2. In this study, three different techniques (micro-GC, infrared, and Raman spectroscopies) were deployed on an experimental flooded borehole for monitoring purposes after CO_2 injection. The aim was to develop a real-time chemical monitoring device to follow dissolved gas concentrations by measurements in water inside the borehole but also at the surface through a gas collection system in equilibrium with the borehole water. However, all three techniques must be calibrated to provide the most accurate quantitative data. For this, a first step of calibration in the laboratory was carried out. A new calibrations were required to determine partial pressure and/or concentrations of gases in water or in the gas collection system. For gas phase analysis, micro-GC, FTIR spectroscopy, and Raman spectroscopy were compared. New calibration of the micro-GC was done for CO_2, CH_4, and N_2 with uncertainty from ±100 ppm to 1.5 mol% depending on the bulk concentration and the type of gas. The FTIR and Raman spectrometers were previously calibrated for CO_2, and CO_2, N_2, O_2, CH_4, and H_2O, respectively with an accuracy of 1–6% depending on concentration scale, gas and spectrometer. Dissolved CO_2 in water was measured using a Raman spectrometer equipped with an immersion probe. The uncertainty on the predicted dissolved CO_2 concentration and partial pressure was ±0.003 mol·kg^{-1} and ±0.05 bar, respectively.

Keywords: Chemical monitoring, Multi-sensors, CO_2 injection, Dissolved gas, Calibration.

1 Introduction

Since the last decades, research projects related to the monitoring of the underground gas content within a borehole are still a topical subject that is directly involved in several environmental preservation applications. For instance, in the face of global warming and climate change, numerous Carbon Capture, Utilization, and Storage projects (CCUS) are performed around the world [1, 2] to reduce the anthropogenic greenhouse gas emission into the atmosphere such as the Century Plant CCUS project in the USA, the Sleipner CCS project in Norway [3], the Shenhua CCUS project in China [4], and the Lacq-Rousse CCS project in France [5, 6], etc. Within such application, the monitoring strategy of the soil gas content variation must be deployed before CO_2 injection (to establish the baseline concentration variation and to define the alert limitation) and during and after CO_2 injection (to detect as soon as possible any CO_2 leakage and environmental impacts). The geological sequestration of nuclear waste also received huge attention from the scientific community with many studies in which the confining properties of the host rock of the geological storage site were investigated to assess its long-term safety [7–10]. For that, the evolution of the concentration of dissolved gases (CO_2, CO, CH_4, C_2H_6, C_3H_8, N_2, H_2, O_2, H_2S, etc.) in the pore water is the key information to understanding the fluid-rock interaction mechanisms and the transport properties of solutes within the host rock [8, 10].

Intense efforts have been made on the metrological development including the optimization of the experimental protocol and the data processing or the enhancement of the accuracy of the measurement [8, 11–14]. Since the chemical composition of the (dissolved) gases within the underground medium is not fully known prior, the combination

* Corresponding author: marie-camille.caumon@univ-lorraine.fr

of different techniques is envisaged in order to detect and quantify *in-situ* and continuously as much gas as possible. Nowadays, the Fourier Transform InfraRed (FTIR) and the Raman vibrational spectroscopies are widely used for continuous measurement of natural gas analyses [14–18]. Quantitative measurement using vibrational spectroscopy is not a straightforward analysis but requires first precise calibration of the signal of each gas with respect to the properties of interest (*e.g.*, molar proportion, partial pressure). Since the signal from vibrational spectroscopy is particularly sensitive to different instrumental parameters (excitation wavelength, response function of the device) as well as the operational environmental conditions (pressure, temperature), the calibration is therefore device-specific and should be regularly re-calibrated to ensure the highest accuracy of measurement. It is to note that FTIR spectroscopy presents some intrinsic limitations. For instance, the spectra of the combination band of CO_2 (centered at 3610 cm^{-1}) are strongly affected by the H_2O vapor contribution at some concentration ranges and required specific additional processing [16]. Also, the homonuclear diatomic gases (such as N_2, O_2) cannot be detected by FTIR spectroscopy whereas they are an important indicator of the biological activity of the soil (*e.g.*, soil respiration processes) and the oxygenation conditions [17, 19–22]. On the other hand, the Raman technique can detect the most common natural gases (including CO_2, CH_4 as well as H_2, O_2, and N_2...) but with a lower sensitivity compared to that of FTIR spectroscopy. Combining these two techniques can thus bring interesting and complementary information to each other. Besides, the micro gas chromatograph (micro-GC), which is a molecular separative technique, is a powerful technique with very high sensitivity and reproducibility for natural gas analyses. Using at least two modules with two different columns and carrier gas, all the pre-cited gases can be analyzed.

The *in-situ* and continuous measurement of the dissolved gas concentration within an aquifer or the aqueous phase of the borehole is still challenging due to the technical limitation of the instruments (*e.g.*, low sensitivity of the Raman spectroscopy, the lack of accurate calibration data). Assuming that the partial pressures of the gases dissolved within the liquid and the gaseous phases above the liquid are in equilibrium [23], the dissolved gas concentration with an aquifer or a flooded borehole can be thus indirectly measured by analyzing its gaseous form. For this purpose, the specific polymeric membrane-based completion SysMoG designed by Solexperts was developed which permitted the collection of gaseous species in equilibrium with dissolved species but excluded water [5]. The collected dissolved gases can thereby be transported from the aquifer or the flooded depth borehole *via* a gas circulation system to different analytical techniques to be analyzed. Besides, the dissolved concentration or the partial pressure of CO_2 can also be derived from the pore water *ex-situ* analysis, *e.g.*, calculated from the measured alkalinity or the total inorganic carbon content using PHREEQC software [8, 24]. However, the pore water extraction requires a careful sampling procedure to avoid any sample chemical alteration (due to the contact with the atmosphere for example) which in turn may result in an error of the measured dissolved gas concentration. In a previous study [8], there was a noticeable discrepancy between the partial pressure of dissolved CO_2 measured in the gaseous phase and the one calculated from water composition in sampled water which could not be fully interpreted. Thus, more experiments are still needed to investigate the gas membrane transfers to better interpret the evolution of the dissolved gas concentration. For this purpose, an experimental borehole of 51-meter depth drilled by Solexperts is devoted to developing and testing the experimental protocol and new analytical instruments before deploying them in the field. The borehole is equipped with a specific membrane-based completion SysMoG and a closed gas circulation system which allows continuous gas analysis by different techniques. Several CO_2 injections into water within the borehole were performed to simulate CO_2 leakage. The micro-GC, Raman, and FTIR spectroscopies are connected all together to the gas circulation system to do the *in-situ* analysis.

The purpose of this study is to calibrate and compare the performance of the instruments in quantifying dissolved gases before using them online with the instrumented borehole. Here the calibration procedure and the new calibration data for the quantitative analysis of CO_2, CH_4, and N_2 concentrations are detailed. The application of these calibrations to the measurement in the borehole during CO_2 injection will be published in a dedicated paper [25].

2 Material and methods

2.1 Description of the experimental borehole

The experimental site consists of a borehole of 51-meter depth and 10 cm in diameter, drilled by Solexperts (Vandœuvre-lès-Nancy, France). The borehole is entirely isolated from its surrounding medium, *i.e.*, there is no contact between the borehole and the adjacent soil or the groundwater. The piezometer level within the borehole is freely adjusted by adding or removing water. The hydrostatic pressure at the bottom of the borehole is ~3–5 bars and the temperature is ~10 °C. For the *in-situ* continuous measurement of the gas concentration, a SysMoG completion is installed into the borehole and connected to the analytical instruments placed at the ground *via* a gas circulation system.

The gases dissolved in the aqueous phase equilibrate across the hydrophobic membrane into a Gas Collection Chamber (GCC) (Fig. 1). A gas circulation line connects the GCC of the completion to the analytical module placed at the ground in a closed system. The analytical instruments are set up at the ground including an FTIR spectrometer, a micro gas chromatograph (micro-GC), and two Raman spectrometers for continuous monitoring of the concentration of the different gases (*e.g.*, CO_2, CH_4, N_2, O_2, and H_2O). One Raman spectrometer is equipped with an immersion probe to directly measure gas concentration dissolved in water inside the borehole. The other instruments, *i.e.* FTIR, micro-GC, and the second Raman spectrometer, are used to analyze the gases from the gas collection chamber.

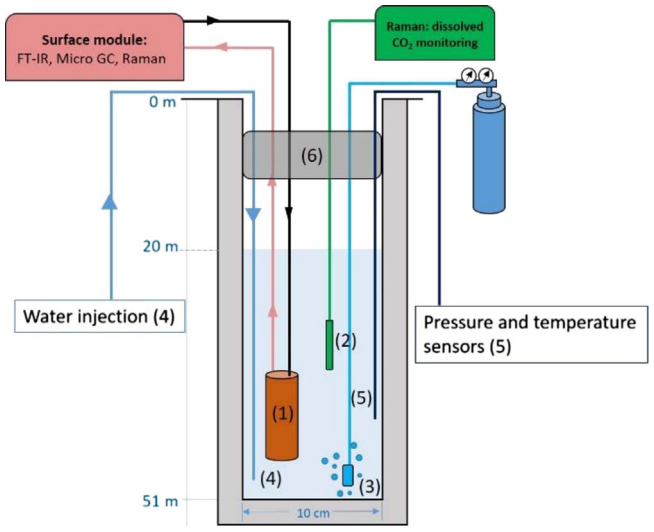

Fig. 1. Schematic drawing of the instrumented borehole. (1) The gas collection chamber connected to surface instruments; (2) Raman probe for dissolved gases; (3) gas injector; (4) water injector; (5) pressure and temperature sensor and (6) packer isolating the flooded area from the air.

2.2 Laboratory experimental setup to determine dissolved CO_2 concentration by Raman spectroscopy

The signal of the Raman RNX2 spectrometer (Kaiser Optical Systems) coupled with an immersion probe (WetHead™) is calibrated to determine the concentration of CO_2 dissolved in water. It is done by acquiring the Raman spectra of a water solution equilibrated with a known pressure of CO_2 at a known temperature. Indeed, according to Henry's law [23] the concentration of a gas dissolved in a solution at equilibrium is proportional to its partial pressure within the vapor phase, which is above the liquid phase and can be calculated by equation (1):

$$C_{CO_2} = K_H^{\circ} \cdot p, \tag{1}$$

where C_{CO_2} is the concentration of the dissolved CO_2 ($mol \cdot kg^{-1}$), p is the partial pressure of CO_2 in a gaseous phase, K_H° is Henry's law constant for the solubility of CO_2 at 298.15 K, (*i.e.*, $K_H^{\circ} = 0.034$ $mol \cdot kg^{-1} \cdot bar^{-1}$) [26]. The Henry's law constant at a given temperature T (K_H^T) can be calculated by K_H° using equation (2):

$$K_H^T = K_H^{\circ} \cdot \exp\left(2400 \cdot \left(\frac{1}{K} - \frac{1}{298.15}\right)\right). \tag{2}$$

The Raman spectra of CO_2 dissolved in water at different equilibrium states are recorded by using the experimental setup shown in Figure 2. The calibration apparatus consists of a 1000-mL airtight stainless-steel cylinder (Swagelok, Fig. 2.1) in which ultrapure Milli-Q water is equilibrated with CO_2 at controlled pressures. One end of the cylinder is connected by a union cross (Swagelok) and three valves to a pump (Fig. 2.2), a pressure transducer (Fig. 2.3), and a bottle of CO_2 (Fig. 2.4). The three valves are firstly closed and the cylinder is then inversed and fill with about 500 ml of water into the cylinder *via* its bottom end (Fig. 2.5). The immersion probe is then inserted into the cylinder in a way to ensure that the head of the immersion probe is still under the water level when the cylinder is closed and inversed again (Fig. 2.6). The cylinder is closed by a specific for ensuring there is no gas or water leakage and then vertically fixed with a stand. The Raman probe is connected to a Raman RXN2 spectrometer (Fig. 2.7) by a 100-m long optical fiber. Before introducing CO_2 into the cylinder, the entire system is evacuated under a vacuum to remove the air inside the cylinder. Once the purge is done, CO_2 is introduced into the cylinder at the desired pressure *via* the gas inlet (Fig. 2.4) by using a pressure regulator connected to the compressed CO_2 bottle (99.99% purity, Air Liquid). The internal pressure is monitored by the pressure transducer (Fig. 2.3). Room temperature is also monitored. Thus CO_2 gradually dissolves into water at controlled conditions (P and T).

CO_2 and H_2O Raman spectra are simultaneously recorded over the spectral range 1350–1850 cm^{-1} with the Raman RXN2 spectrometer. The wavelength and power of the excitation radiation are 532 nm and ~100 mW, respectively. The acquisition time is 30 s per accumulation and 3 accumulations for each measurement. An example of spectra of CO_2 dissolved in water is shown in Figure 3. The obtained spectra were then processed by LabSpec6 software (Horiba) to determine the peak area of CO_2 and H_2O after baseline subtraction. As the area of the lower band of CO_2 at ~1285 cm^{-1} is too small, only the area of the upper band of CO_2 at ~1381 cm^{-1} was considered. Besides, the Raman H–O–H bending mode of water is observed over a spectral range from 1450 to 1800 cm^{-1} which superimposes the signal of the sapphire windows of the immersion probe at ~1522 cm^{-1} (Fig. 3). Thus, the total peak area of the H_2O band was calculated after subtracting the signal of sapphire.

The internal pressure of the tanker was firstly set at ~2 bars. The time needed to reach the equilibrium is more than 3 days (Fig. 5). When pressure increases from 2 bars (at equilibrium) to 3 bars, the time needed to reach the new equilibrium state at 3 bars is less than one day. Afterward, the pressure is successively decreased to ~2.5, 1.5, 1, 0.7, 0.5, 0.3, and 0.1 bar by adjusting the pressure regulator of the gas bottle and/or opening the valve (Fig. 2.4). The equilibrium state at these lower pressures is reached after few hours. Shaking of the entire tanker can help to speed up the equilibrium process.

2.3 Determination of the concentrations in the gas phase

2.3.1 Micro-GC calibration

The micro-GC-490 (Agilent) was calibrated for the quantitative measurement of CO_2, CH_4 and N_2. CH_4 and N_2 were quantified using a module with a Molsieve 5Å column (10 m) with argon as carrier gas and CO_2 using the module with a PoraplotU column (10 m) with helium as carrier gas.

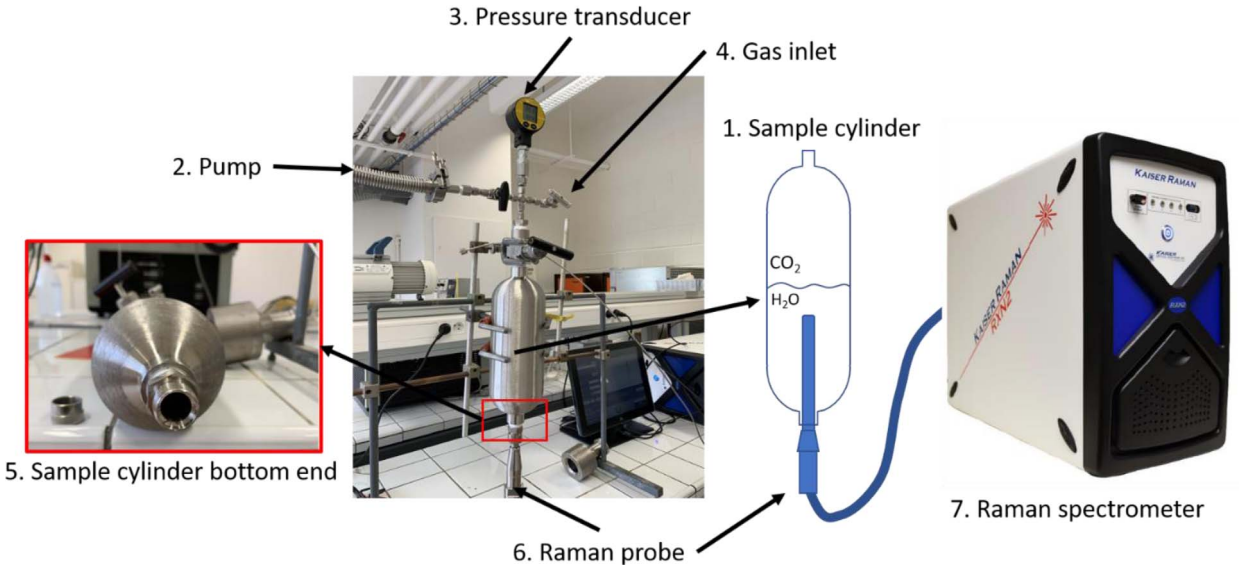

Fig. 2. Experimental setup to measure the Raman signal of dissolved CO_2 as a function of pressure. (1) 1000-mL stainless-steel cylinder. The upper end of the cylinder is connected to a pump (2), a pressure transducer (3), and a bottle of pure compressed CO_2 (4). The Raman probe (6) is introduced *via* the other end of the cylinder which is then closed by a special tor to ensure there is no water leakage. The Raman probe is connected to a Raman RXN2 spectrometer (7) by a 100-m optical fiber.

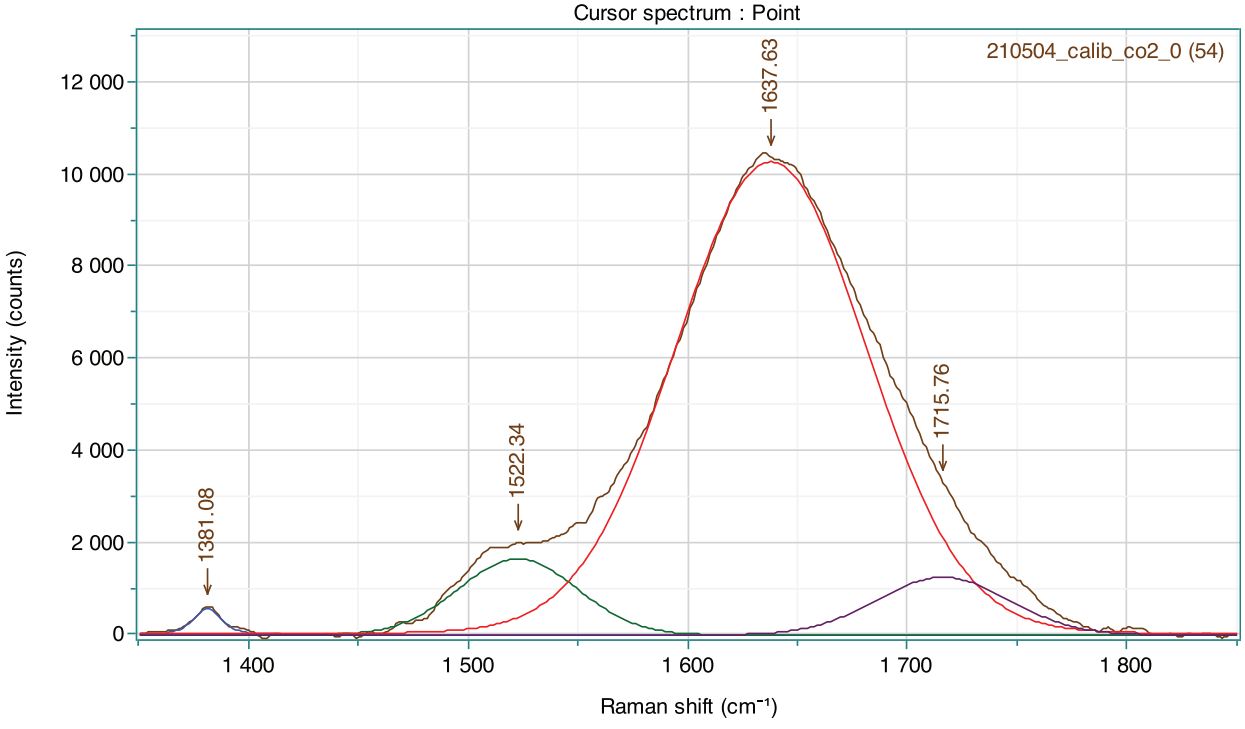

Fig. 3. Raman spectra of CO_2 dissolved in water under a pressure of 0.75 bar after baseline subtraction and peak fitting. The upper band of the CO_2 Fermi diad is observed at 1381 cm^{-1}. The H–O–H bending mode of H_2O is observed in the range 1450–1800 cm^{-1}.

For the two modules, the injection time is 50 ms, the injector temperature is 90 °C, the carrier gas pressure is 30 psi (~2 bar) and the detectors are micro catarometer (μTCD). The column temperature is 145 °C for the Molsieve module and 80 °C for the PoraplotU module. Peak integration is done with Soprane Software (SRA). Calibrations were established using reference gases of known concentration (commercial standard gases with certified concentration, the uncertainty is less than 1%) or gas mixtures prepared in the laboratory from pure gases by using a gas mixer

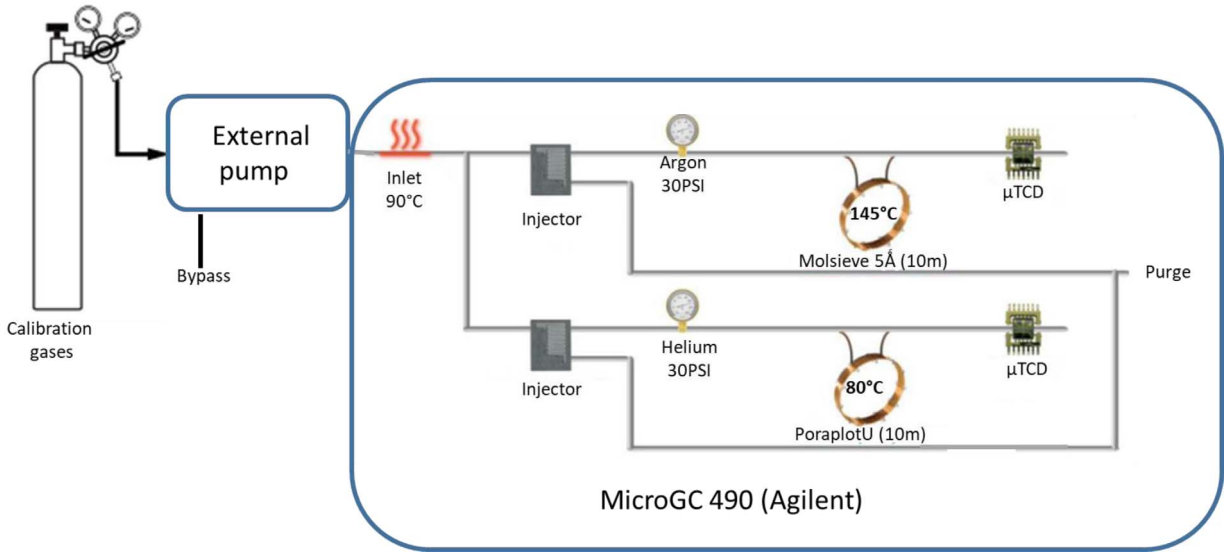

Fig. 4. Simplified scheme describing the gas circulation within the micro-GC 490.

(GasMix™-AlyTech). The uncertainty on the concentration of the prepared gas mixtures is less than 3%. To ensure the highest accuracy of the calibration data at a low concentration range, the concentrations of CO_2 and CH_4 of some prepared gas mixtures, when below 4000 ppm, are re-checked by the G2201-i analyzer (Picarro, Inc.).

Upon the calibration procedure, the entrance of the micro-GC is directly connected to the bottle of standard gas or the outlet of the AlyTech gas mixer (Fig. 4). To introduce the gases into the micro-GC, an external pump is used and turned on for about 20 s to remove any atmospheric air in the system. Once this is done, the reference gases are introduced at a pressure of less than 1.5 bar. Thereby, the whole volume of the external pump and connecting tubes is filled only by the reference gas. The reference gas is then injected into the analysis modules to be analyzed thanks to the internal pump (Fig. 4).

2.3.2 FTIR spectrometer calibration

The IR measurements are performed using a portable FTIR Bruker Alpha spectrometer (Bruker Optics GmbH, Germany) equipped with a 5 cm path-length stainless-steel gas cell. The latter is equipped with two ZnSe (Zinc Selenide) windows and is directly connected to the gas circuit for continuous measurement of gas concentration. The IR spectra are scanned 16 times over the spectral range 600–4000 cm^{-1}.

The calibration data of the FTIR apparatus used herein (including the spectrometer and the gas cell) for the quantification of CO_2 concentration over a range from 100 to 60,000 ppm was established in previous work (see Fig. 4 in [22]). The calibration curve links the CO_2 concentration (ppm) to the variation of the peak area of the fundamental band ν_3 of CO_2 at ~2350 cm^{-1}. According to the authors, the accuracy of the CO_2 concentration measurement is less than 6% at <2000 ppm, less than 4% up to 5000 ppm, less than 2% up to 30,000 ppm, and less than 1% up to 100,000 ppm.

Table 1. Raman peak position and corresponding scattering cross-section (σ) for an excitation wavelength of 532 nm [28–31].

	Peak position (cm^{-1})	σ
CO_2 (upper band)	1388	1.54
CH_4	2917	7.73
N_2	2331	1
O_2	1555	1.24
H_2	4153	2.3
H_2O vapor	3665	2.35

2.3.3 Raman spectrometer calibration

The molar fraction (X_i, mol%) of gaseous species within a mixture can be determined from the Raman scattering cross-section (σ_i) of the vibrational mode of gases and the corresponding peak area (A_i) by using equation (3) [27]:

$$X_i = \frac{\left(\frac{A_i}{\sigma_i \zeta_i}\right)}{\sum_{1}^{i}\left(\frac{A_i}{\sigma_i \zeta_i}\right)}, \quad (3)$$

where ζ_i is the instrumental efficiency which depends on the wavelength (peak position). As the spectrometer intensity response was calibrated using a reference emission lamp (HCA, Kaiser Optical System), all ζ_i was equal for all gases. Therefore, the σ_i values from the literature of N_2, CO_2, CH_4, O_2, and H_2O for the excitation wavelength of 532 nm can be used [28–31] (Tab. 1)

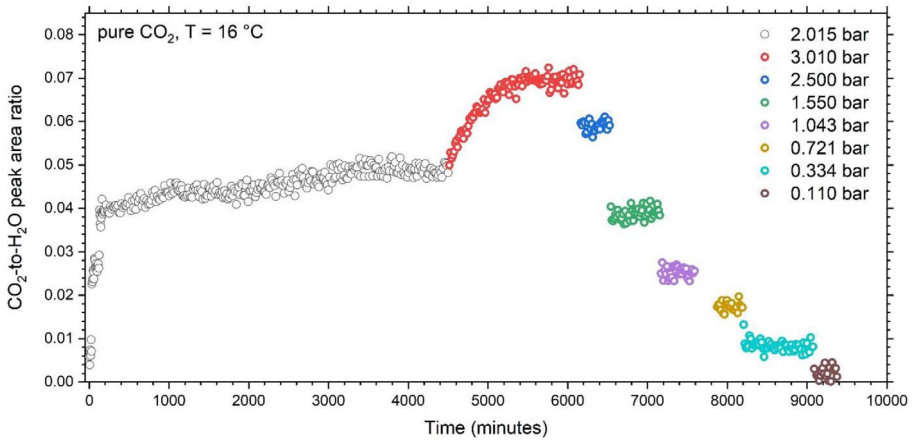

Fig. 5. Evolution of carbon dioxide-to-water peak area ratio (A_{CO_2}/A_{H_2O}) as a function of time (minutes) and pressure (bar).

Table 2. PAR as a function of pressure and CO_2 concentration.

Partial pressure of CO_2 (bar)	Dissolved CO_2 concentration[a] (mol/kg)	Average peak area ratio[b] (A_{CO_2}/A_{H_2O})	Standard deviation
3.010	0.1315	0.06957	0.00120
2.500	0.1092	0.05905	0.00116
2.015	0.0880	0.04874	0.00139
1.550	0.0677	0.03872	0.00134
1.043	0.0456	0.02527	0.00121
0.721	0.0315	0.01740	0.00102
0.334	0.0146	0.00794	0.00094
0.115	0.0048	0.00218	0.00126

[a] Calculated from pressure and temperature using Henry's law constant.
[b] The average peak area ratio is calculated from all experimental data points at equilibrium (Fig. 5). The calibration curve is fitted from all experimental data points, linking the variation of the PAR to the concentration of the dissolved CO_2 (Fig. 6a) or the partial pressure of the CO_2 (Fig. 6b). The uncertainty (1σ) of the predicted CO_2 dissolved concentration and the partial pressure are ± 0.003 mol·kg^{-1} and ± 0.05 bar, respectively.

The Raman measurements of the gases flowing within the gas circulation lines are performed using a Raman RXN1 spectrometer equipped with a 532 nm Nd-YAG excitation laser and coupled with a gas probe (AirHead™, Kaiser Optical Systems, Inc.) *via* a 5-meter-long optical fiber. The air probe is embedded in a dedicatedly designed stainless steel gas cell equipped with a sapphire window and an array of mirrors to amplify the Raman scattering intensity that is connected to the gas circulation systems. The Raman analyses can be thereby continuously performed without changing the internal pressure and the composition of the collected gases. The peak area of the studied gases is measured by integrating their Raman spectrum over a predefined spectral interval, *i.e.*, between 1380 cm^{-1} and 1397 cm^{-1} for the upper band of CO_2 (at 1388 cm^{-1}), between 2319 cm^{-1} and 2341 cm^{-1} for the N_2 band, between 1545 cm^{-1} and 1566 cm^{-1} for O_2, and from 3637 cm^{-1} to 3665 cm^{-1} for H_2O.

3 Calibration data for quantitative measurements

3.1 Quantifying dissolved CO_2 concentration by Raman spectroscopy

The evolution of the CO_2-to-H_2O Peak Area Ratio (PAR) as a function of time is presented in Figure 5. In general, the PAR increases gradually with time following the increase of the amount of dissolved CO_2, then becomes unchanged once the equilibrium state is reached. The average value of PAR at each equilibrium state and its standard deviation are reported in Table 2 with the corresponding concentration of CO_2.

The calibration curves are fitted from all experimental data points, linking the variation of the PAR to the concentration of the dissolved CO_2 (Fig. 6a) and the partial pressure of the CO_2 (Fig. 6b). The uncertainty (1σ) of the

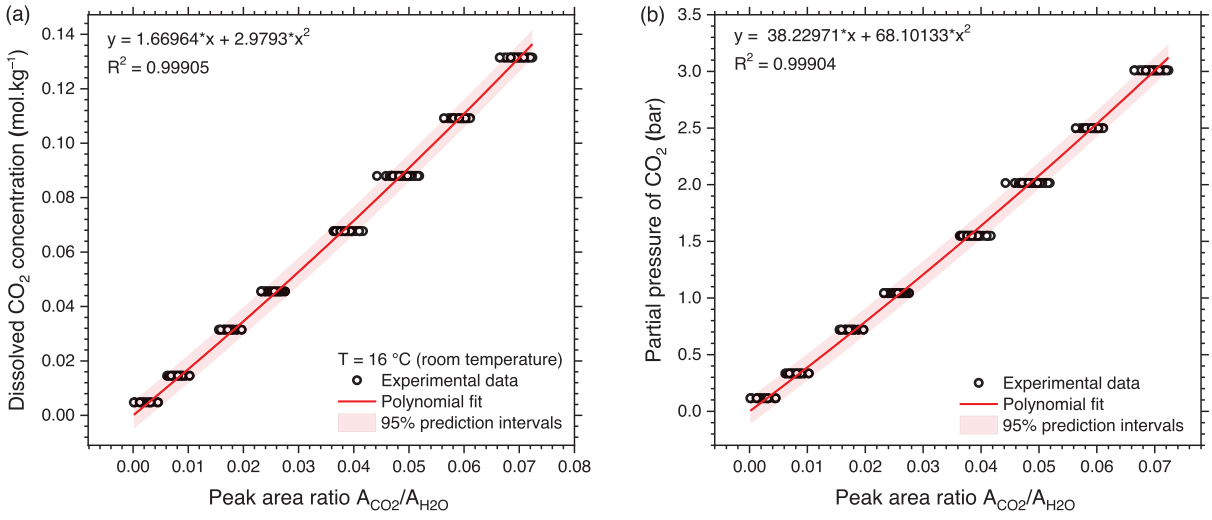

Fig. 6. Relationship between the peak area ratio A_{CO_2}/A_{H_2O} (PAR) and (a) the concentration of CO_2 dissolved in water or (b) CO_2 partial pressure.

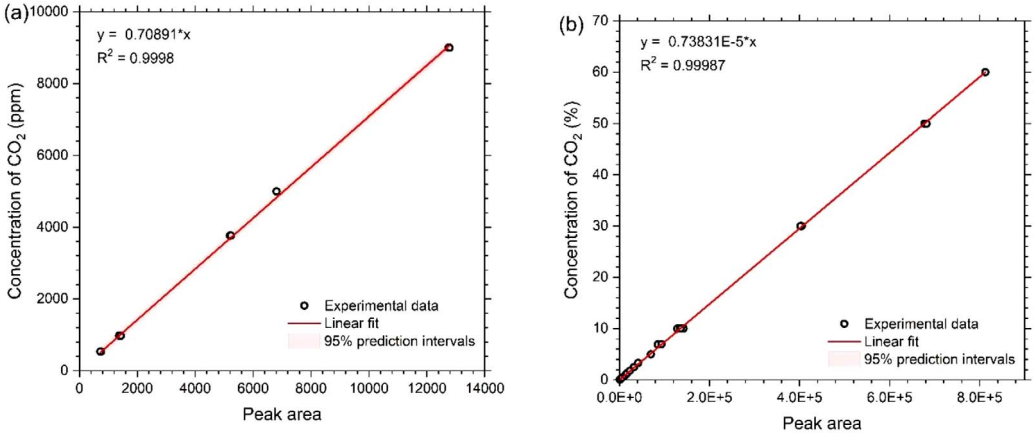

Fig. 7. Calibration of CO_2 signal for (a) low and (b) intermediate concentration range, *i.e.*, <9000 ppm and <60 mol%, respectively.

predicted dissolved CO_2 concentration and the partial pressure is about ±0.003 mol·kg^{-1} and ±0.05 bar, respectively.

3.2 Gas concentration determined by Micro-GC

In general, the calibration curves of the micro-GC-490 are a linear correlation between the peak area and the concentration (ppm). The signal saturates when the CO_2 concentration is above 60 mol%. Consequently, in the present study, only two calibration curves of CO_2 are provided for low (from 500 to 9000 ppm) and intermediate concentration ranges (up to ~60%) (Fig. 7). The uncertainty of the predicted CO_2 concentration (at 1σ, estimated from the prediction intervals of the regression equation) is less than ±100 ppm for the concentration range under 9000 ppm, <±1000 ppm for the concentration range under 100,000 ppm, and <±0.5% for the concentration range under 60 mol%.

In the same way, calibration data was established over a concentration range from 0 to 5000 ppm for CH_4, and from 1 to 100% for N_2 (Fig. 8). The uncertainty of the predicted concentration of CH_4 and N_2 (1σ, estimated from the prediction intervals) is less than about ±100 ppm and 1.5 mol%, respectively.

3.3 Gaseous CO_2 concentration determined by FTIR

In the present study, the CO_2 concentration within the gaseous phase of the borehole is expected to range from about 500 ppm (near the atmospheric concentration) to 60 mol%. Since the intensity of the IR fundamental band of CO_2 at ~2350 cm^{-1} is quickly saturated above 60,000 ppm, the peak area of the combination bands of CO_2 at ~3610 cm^{-1} ($\nu_1 + \nu_3$ and $2\nu_2 + \nu_3$) is therefore used. It is noted that there is an interference between the IR spectra of the combination bands of CO_2 and that of H_2O vapor around 3610 cm^{-1}. The subtraction of the signal of H_2O vapor from that of CO_2 is thus required to ensure the highest accuracy of the concentration measurement. More details about FTIR data processing can be found in Taquet *et al.* [14]. Moreover, it is also to note that the existing calibration data of the FTIR Alpha spectrometer was

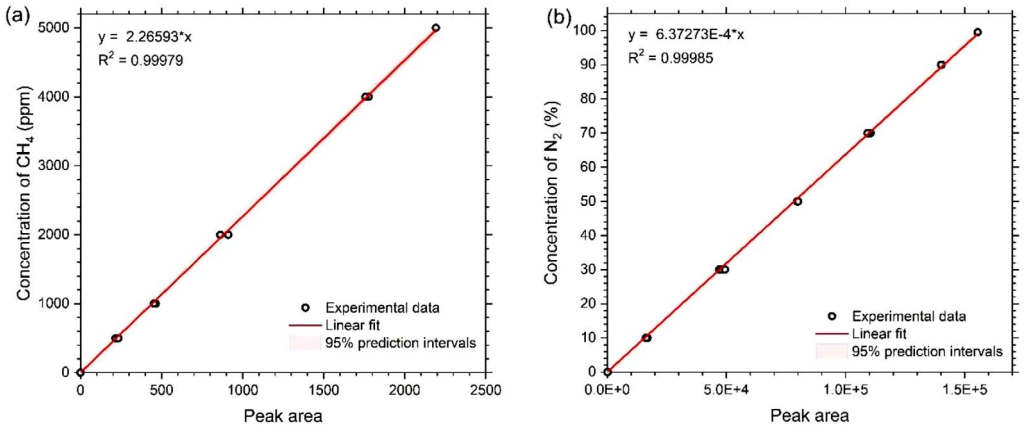

Fig. 8. Calibration data of (a) CH_4 for a concentration range from 0 to 5000 ppm or (b) N_2 for a concentration range from 0 to 100 mol%.

usually established at atmospheric pressure, whereas the intensity and the area of the IR spectra vary as a function of pressure. In this study, the total pressure within the gas circulation system is however expected to vary from the atmospheric pressure to ~up to 2–3 bars due to a large amount of CO_2 dissolved in the aqueous phase, then penetrating across the membrane into the GCC. The calibration data for such a wide pressure and concentration range is not available yet. In the borehole, the FTIR spectra are simultaneously recorded with Raman and micro-GC whose intensity does not depend on the total pressure. Therefore, new calibration curves linking the IR peak area of the combination band of CO_2 to the concentration measured by other techniques (Raman and micro-GC) are thereby established for the pressure and concentration range encountered in the borehole by comparison with Raman spectroscopy and GC [25].

3.4 Gas concentration determined by Raman spectroscopy

Partial pressure and mol% in the gas mixture are determined by Raman spectroscopy using literature data (Tab. 1) and pressure measurement. Previous works using the same Raman spectrometer and the same probe reported uncertainties of about 0.5–1 mol% at atmospheric pressure [14, 18]. The detection limit depends on the cross-section of each gas: the best detection limit is for CH_4 and the lowest one for N_2 (Tab. 1) at about 0.002 mbar and 0.01 mbar, respectively.

4 Conclusion

In preparation for on-site measurement of gas concentration in a flooded borehole, laboratory calibrations are carried out for micro-GC, FTIR spectroscopy, and Raman spectroscopy. Raman spectroscopy is the only of the three techniques able to quantitatively measure the concentration of CO_2 dissolved in water, with an accuracy of 0.003 mol·kg^{-1} or 0.05 bar for the corresponding partial pressure in equilibrium with the solution. For the gas phase, Raman spectroscopy can detect all the studied gases (CO_2, CH_4, N_2, O_2, H_2, H_2O) with an accuracy better than 1 mol % and a detection limit lower than 0.01 mbar. The Micro-GC is calibrated to quantify CO_2, CH_4, and N_2 with a quite much lower detection limit (<100 ppm) and higher accuracy (100 ppm – 5% depending on the concentration range) (*i.e.* 0.2 mbar – 0.1 bar at 2 bar of total pressure). Finally, FTIR can quantify CO_2 concentration in the gas phase over the full concentration range (500 ppm – 100%) with accuracy depending on the concentration range (1–6%, *i.e.*, 0.02–0.12 bar at 2 bar of total pressure). At concentrations higher than 60 mol% and pressure higher than atmospheric pressure, the infrared spectrometer is not yet calibrated. The next acquisition in the flooded borehole will lead to a new calibration in this high-level range by comparison with micro-GC and Raman spectroscopy data [25]. The performance and applicability of each technique and the SysMoG polymeric membrane responsivity and resistance over a wide concentration-pressure range will be evaluated and compared during the measurement run on the instrumented borehole.

Acknowledgments. The authors would like to thank the GEODERNERGIES (Scientific Interest Group), for its financial support through the OUROBOROS (2019–2021) research program.

References

1 Bui M., Adjiman C.S., Bardow A., Anthony E.J., Boston A., Brown S., Fennell P.S., Fuss S., Galindo A., Hackett L.A., Hallett J.P., Herzog H.J., Jackson G., Kemper J., Krevor S., Maitland G.C., Matuszewski M., Metcalfe I.S., Petit C., Puxty G., Reimer J., Reiner D.M., Rubin E.S., Scott S.A., Shah N., Smit B., Trusler J.P.M., Webley P., Wilcox J., Dowell N.M. (2018) Carbon capture and storage (CCS): the way forward, *Energy Environ. Sci.* **11**, 5, 1062–1176.

2 Li H., Jiang H.-D., Yang B., Liao H. (2019) An analysis of research hotspots and modeling techniques on carbon capture and storage, *Sci. Total Environ.* **687**, 687–701.

3 Solomon S. (2006) *Carbon dioxide storage: geological security and environmental issues – case study on the Sleipner gas field in Norway*, The Bellona Foundation, Oslo, Norway.
4 Li Q., Liu G., Liu X., Li X. (2013) Application of a health, safety, and environmental screening and ranking framework to the Shenhua CCS project, *Int. J. Greenh. Gas Control* **17**, 504–514.
5 Taquet N. (2012) *Monitoring Geochimique de la geosphère et de l'atmosphère : application au stockage geologique du CO_2.*
6 Monne J., Prinet C. (2013) Lacq–Rousse industrial CCS reference project: description and operational feedback after two and half years of operation, *Energy Procedia* **37**, 6444–6457.
7 Rübel A.P., Sonntag C., Lippmann J., Pearson F.J., Gautschi A. (2002) Solute transport in formations of very low permeability: profiles of stable isotope and dissolved noble gas contents of pore water in the Opalinus Clay, Mont Terri, Switzerland, *Geochim. Cosmochim. Acta* **66**, 8, 1311–1321.
8 Vinsot A., Appelo C.A.J., Cailteau C., Wechner S., Pironon J., De Donato P., De Cannière P., Mettler S., Wersin P., Gäbler H.-E. (2008) CO_2 data on gas and pore water sampled in situ in the Opalinus Clay at the Mont Terri rock laboratory, *Phys. Chem. Earth Parts A/B/C* **33**, S54–S60.
9 Gaucher E.C., Tournassat C., Pearson F.J., Blanc P., Crouzet C., Lerouge C., Altmann S. (2009) A robust model for pore-water chemistry of clayrock, *Geochim. Cosmochim. Acta* **73**, 21, 6470–6487.
10 Bossart P., Bernier F., Birkholzer J., Bruggeman C., Connolly P., Dewonck S., Fukaya M., Herfort M., Jensen M., Matray J.-M., Mayor J.C., Moeri A., Oyama T., Schuster K., Shigeta N., Vietor T., Wieczorek K. (2017) Mont Terri rock laboratory, 20 years of research: introduction, site characteristics and overview of experiments, *Swiss J. Geosci.* **110**, 1, 3–22.
11 Laier T., Øbro H. (2009) Environmental and safety monitoring of the natural gas underground storage at Stenlille, Denmark, *Geol. Soc. Spec. Publ.* **313**, 1, 81–92.
12 de Donato P., Pironon J., Mouronval G., Hy-Billiot J., Garcia B., Lucas H., Pokryszka Z., Lafortune S., Flamant P.H., Cellier P., Gal F., Pierres K.M.-L., Pierres K.L., Taquet N., Barres O. (2010) SENTINELLE. Development of combined geochemical monitoring on Lacq pilot site from geosphere to atmosphere, in: 10th International Conference on Greenhouse Gas Control Technologies (GHGT 10), September 2010, Amsterdam, Netherlands. https://ineris.hal.science/ineris-00970681.
13 Cailteau C., Pironon J., de Donato P., Vinsot A., Fierz T., Garnier C., Barres O. (2011) FT-IR metrology aspects for on-line monitoring of CO 2 and CH 4 in underground laboratory conditions, *Anal. Methods* **3**, 4, 877–887.
14 Taquet N., Pironon J., de Donato P., Lucas H., Barres O. (2013) Efficiency of combined FTIR and Raman spectrometry for online quantification of soil gases: application to the monitoring of carbon dioxide storage sites, *Int. J. Greenh. Gas Control* **12**, 359–371.
15 Dubessy J., Poty B., Ramboz C. (1989) Advances in C–O–H–N–S fluid geochemistry based on micro-Raman spectrometric analysis of fluid inclusions, *Eur. J. Mineral.* **1**, 517–534.
16 Cailteau C., de Donato P., Pironon J., Vinsot A., Garnier C., Barres O. (2011) In situ gas monitoring in clay rocks: mathematical developments for CO_2 and CH_4 partial pressure determination under non-controlled pressure conditions using FT-IR spectrometry, *Anal. Methods* **3**, 4, 888–895.
17 Gal F., Michel K., Pokryszka Z., Lafortune S., Garcia B., Rouchon V., de Donato P., Pironon J., Barres O., Taquet N., Radilla G., Prinet C., Hy-Billiot J., Lescanne M., Cellier P., Lucas H., Gibert F. (2014) Study of the environmental variability of gaseous emanations over a CO_2 injection pilot – application to the French Pyrenean foreland, *Int. J. Greenh. Gas Control* **21**, 177–190.
18 Lacroix E., de Donato P., Lafortune S., Caumon M.-C., Barres O., Liu X., Derrien M., Piedevache M. (2021) In situ continuous monitoring of dissolved gases (N_2, O_2, CO_2, H_2) prior to H_2 injection in an aquifer (Catenoy, France) by on-site Raman and infrared spectroscopies: instrumental assessment and geochemical baseline establishment, *Anal. Methods* 13, 3806–3820.
19 Lloyd J., Taylor J.A. (1994) On the temperature dependence of soil respiration, *Funct. Ecol.* **8**, 3, 315–323.
20 Angert A., Yakir D., Rodeghiero M., Preisler Y., Davidson E. A., Weiner T. (2015) Using O_2 to study the relationships between soil CO_2 efflux and soil respiration, *Biogeosciences* **12**, 7, 2089–2099.
21 Barba J., Cueva A., Bahn M., Barron-Gafford G.A., Bond-Lamberty B., Hanson P.J., Jaimes A., Kulmala L., Pumpanen J., Scott R.L., Wohlfahrt G., Vargas R. (2018) Comparing ecosystem and soil respiration: review and key challenges of tower-based and soil measurements, *Agric. For. Meteorol.* **249**, 434–443.
22 Adisaputro D., De Donato P., Saint-Andre L., Barres O., Galy C., Nourrisson G., Piedevache M., Derrien M. (2021) Baseline subsoil CO_2 gas measurements and micrometeorological monitoring: above canopy turbulence effects on the subsoil CO_2 dynamics in temperate deciduous forest, *Appl. Sci.* **11**, 4, 1753.
23 Henry W., Banks J. (1803) III. Experiments on the quantity of gases absorbed by water, at different temperatures, and under different pressures, *Philos. Trans. R. Soc. London* **93**, 29–274.
24 Vinsot A., Appelo C.A.J., Lundy M., Wechner S., Cailteau-Fischbach C., de Donato P., Pironon J., Lettry Y., Lerouge C., De Cannière P. (2017) Natural gas extraction and artificial gas injection experiments in Opalinus Clay, Mont Terri rock laboratory (Switzerland), *Swiss J. Geosci.* **110**, 1, 375–390.
25 Le, V.-H.; Pironon, J.; De Donato, P.; Piedevache, Médéric; Randi, A.; Lorgeoux, C.; Caumon, M.-C. and Barres, O.: In-situ monitoring of dissolved gases within flooded borehole by multiples techniques (Raman, FTIR, micro-GC). Assessing of the gas membrane transfer equilibrium, (in prep.).
26 Mackay D., Shiu W.Y. (1981) A critical review of Henry's law constants for chemicals of environmental interest, *J. Phys. Chem. Ref. Data* **10**, 4, 1175–1199.
27 Pasteris J.D., Wopenka B., Seitz J.C. (1988) Practical aspects of quantitative laser Raman microprobe spectroscopy for the study of fluid inclusions, *Geochim. Cosmochim. Acta* **52**, 5, 979–988.
28 Schrötter H.W., Klöckner H.W. (1979) Raman scattering cross section in gases and liquids, in: Weber A. (Ed.), *Raman spectroscopy of gases and liquids, topics in current physics.* Springer Berlin Heidelberg, Berlin, pp. 123–164.
29 Burke E.A.J. (2001) Raman microspectrometry of fluid inclusions, *Lithos* **55**, 1, 139–158.

30 Le V.-H., Caumon M.-C., Tarantola A., Randi A., Robert P., Mullis J. (2019) Quantitative measurements of composition, pressure and density of micro-volumes of CO_2–N_2 gas mixtures by Raman spectroscopy, *Anal. Chem.* **91**, 22, 14359–14367.

31 Le V.-H., Caumon M.-C., Tarantola A., Randi A., Robert P., Mullis J. (2020) Calibration data for simultaneous determination of P–V–X properties of binary and ternary CO_2–CH_4–N_2 gas mixtures by Raman spectroscopy over 5–600 bar: application to natural fluid inclusions, *Chem. Geol.* **552**, 119783.